Biosensors and Bioelectronics 61 (2014) 227–231

Contents lists available at ScienceDirect

Biosensors and Bioelectronics

journal homepage: www.elsevier.com/locate/bios

Performance characterization of an abiotic and fluorescent-based continuous glucose monitoring system in patients with type 1 diabetes

Mark Mortellaro*, Andrew DeHennis

Senseonics, Incorporated, 20451 Seneca Meadows Parkway, Germantown, MD 20876, United States

ARTICLE INFO

Article history:
Received 24 February 2014
Received in revised form
6 May 2014
Accepted 8 May 2014
Available online 17 May 2014

Keywords:
Continuous glucose monitoring
Fluorescent sensor
Implantable
Boronic acid

ABSTRACT

A continuous glucose monitoring (CGM) system consisting of a wireless, subcutaneously implantable glucose sensor and a body-worn transmitter is described and clinical performance over a 28 day implant period in 12 type 1 diabetic patients is reported. The implantable sensor is constructed of a fluorescent, boronic-acid based glucose indicating polymer coated onto a miniaturized, polymer-encased optical detection system. The external transmitter wirelessly communicates with and powers the sensor and contains Bluetooth capability for interfacing with a Smartphone application. The accuracy of 19 implanted sensors were evaluated over 28 days during 6 in-clinic sessions by comparing the CGM glucose values to venous blood glucose measurements taken every 15 min. Mean absolute relative difference (MARD) for all sensors was 11.6 ± 0.7%, and Clarke error grid analysis showed that 99% of paired data points were in the combined A and B zones.

1. Introduction

The prevalence of diabetes mellitus continues to increase in industrialized countries, and projections suggest that this figure will rise to 4.4% of the global population (366 million individuals) by the year 2030 (Wild et al., 2004). Glycemic control is a key determinant of long-term outcomes in patients with diabetes, and poor glycemic control is associated with retinopathy, nephropathy and an increased risk of myocardial infarction, cerebrovascular accident, and peripheral vascular disease requiring limb amputation (Group, 1998). Despite the development of new insulins and other classes of antidiabetic therapy, roughly half of all patients with diabetes do not achieve recommended target hemoglobin A1c (HbA1c) levels < 7.0% (Resnick, 2006).

Frequent self-monitoring of blood glucose is necessary to achieve tight glycemic control in patients with diabetes mellitus, particularly for those requiring insulin therapy (Farmer et al., 2007; Klonoff, 2007). Continuous glucose monitors (CGMs) enable frequent glucose measurements as well as detection and alerting of impending hyper- and hypoglycemic events (Clarke and Kovatchev, 2007). The use of CGMs by type 1 diabetics has been demonstrated to significantly reduce their time spent in hypoglycemia (Battelino et al., 2011). Moreover, integration of CGMs with automated insulin pumps allows for establishment of a closed-loop "artificial pancreas" system to more closely approximate physiologic insulin delivery and to improve adherence (Clarke and Kovatchev, 2007). However, currently available transcutaneous CGM systems have short durations of use and require replacement every 5–7 days (Calhoun et al., 2013; Christiansen et al., 2013; McGarraugh et al., 2011). Sensor in vivo lifetime may be limited by stability of the enzymes used for glucose recognition, by bio-fouling at the surface of the sensor electrodes, by ongoing inflammatory responses surrounding the sensors as a consequence of the partial implantation (i.e., sensor protrudes through the skin), or by a combination of these effects. To overcome these limitations, a fully subcutaneously implantable sensor has been developed that uses a fluorescent, non-enzymatic (bis-boronic acid based) glucose indicating hydrogel and a miniaturized optical detection system.

The present report describes the technology of the continuous glucose monitoring system and presents accuracy and performance data of sensors implanted for 28 continuous days in patients with type 1 diabetes.

2. Materials and methods

2.1. Continuous glucose monitoring system

The components of the novel CGM system are shown in Fig. 1. A small, fully subcutaneously insertable sensor measures glucose concentrations in interstitial fluid. An externally worn transmitter

* Corresponding author. Tel.: +1 301 556 1616; fax: +1 301 515 0988.
E-mail address: mark.mortellaro@senseonics.com (M. Mortellaro).

http://dx.doi.org/10.1016/j.bios.2014.05.022

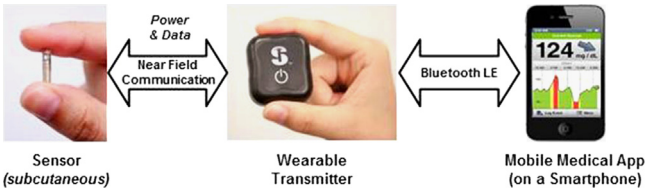

Fig. 1. Continuous glucose monitoring system components.

remotely powers and communicates with the inserted sensor to initiate and receive the measurements. This information is communicated wirelessly via Bluetooth™ to a Handheld Application running on a secondary display and can be downloaded and configured through a Universal Serial Bus (USB) port. A web interface has also been developed for plotting and sharing of uploaded data.

2.1.1. Subcutaneously insertable fluorescent sensor

The sensor (Fig. 2A) is a micro-fluorometer that is encased in a rigid, translucent and biocompatible polymer capsule 3.3 mm [0.13″] in diameter and 15 mm [0.62″] in length (Colvin and Jiang, 2013). Glucose concentration is measured by means of fluorescence from the glucose-indicating hydrogel, which is polymerized onto the capsule surface over the optical cavity. The optical system contained within the capsule is comprised of a light-emitting diode (LED), which serves as the excitation source for the fluorescent hydrogel; two spectrally filtered photodiodes, which measure the glucose-dependent fluorescence intensity; an integrated circuit with onboard temperature sensor; and an antenna, which receives power from and communicates with the transmitter.

The glucose-indicating hydrogel (Fig. 2B) consists primarily of poly(2-hydroxyethyl methacrylate) (pHEMA) into which a fluorescent indicator (Fig. 2C) is copolymerized. In contrast to other CGMs, which utilize electrochemical enzyme-based glucose sensors, no chemical compounds are consumed (i.e., glucose, oxygen) or formed (i.e., hydrogen peroxide) during use, and the glucose-indicating hydrogel is not subject to the instability characteristics of enzymes. Instead, glucose reversibly binds to the indicator boronic acids groups (which act as glucose receptors) in an equilibrium binding reaction (James et al., 2006). Subsequent disruption of photoinduced electron transfer (PET) results in an increased fluorescence intensity upon glucose-binding. When glucose is not present, anthracene fluorescence is quenched by intermolecular electron transfer (indicated by the curved arrows in Fig. 2c) from the unpaired electrons on the indicator tertiary amines. When glucose is bound to the boronic acids, the Lewis acidity of boron is increased, and weak boron-nitrogen bonds are formed. This weak bonding prevents electron transfer from the amines and consequently prevents fluorescence quenching. Of note, the indicator is not chemically altered as a result of the PET quenching process. Fluorescence increases with increasing glucose concentrations until all indicator binding sites are filled at which point the signal reaches a plateau (James et al., 2006; Shibata et al., 2010). The measurement of a given glucose concentration can be modeled by the following equation:

$$Glucose = K_d \frac{F_{meas} - F_{min}}{F_{max} - F_{meas}}, \quad (1)$$

where F_{min} is the integrated fluorescence in the absence of glucose, F_{max} is the integrated fluorescence when all of the accessible indicator is bound to glucose, F_{meas} is the integrated fluorescence at a given concentration of glucose, and K_d is the dissociation constant for the indicator. Eq. (1) serves as the core of the CGM system glucose algorithm that also incorporates kinetic and

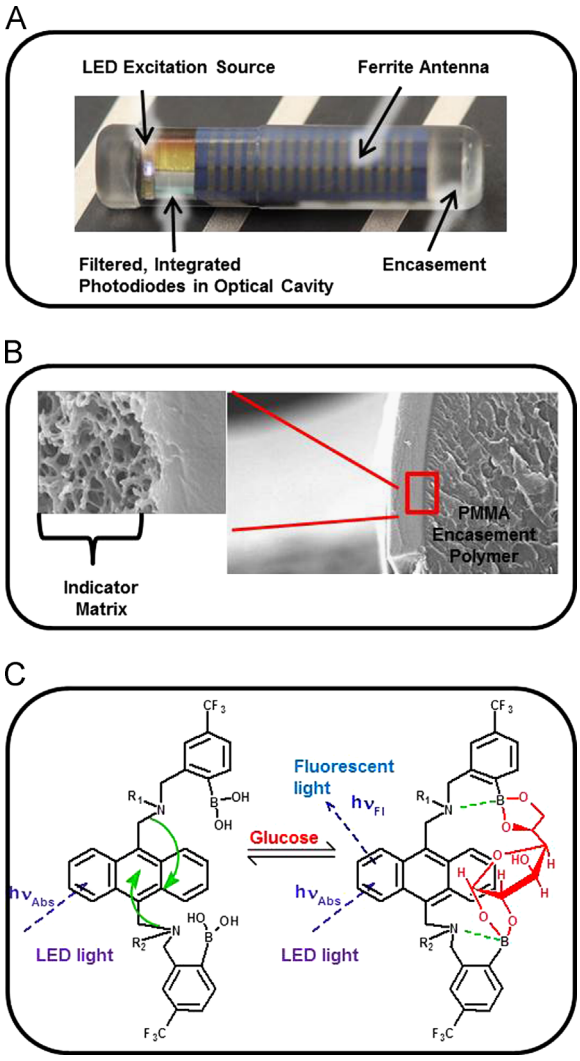

Fig. 2. Implantable optical-based glucose sensor. (A) Photograph of the implantable glucose sensor (shown without glucose-indicator hydrogel coating); (B) scanning electron microscope (SEM) images of the glucose indicator hydrogel grafted onto the outside of the PMMA sensor encasement; and (C) chemical structure and glucose binding mode of indicator moiety. R_2 shown in the figure denotes connectivity to the hydrogel backbone, while R_1 represents a propionic acid side chain.

temperature dependences, as previously described (Wang et al., 2012). Since self-monitored blood glucose (i.e., finger-stick) measurements are used to calibrate the CGM system, a time and glucose dependent lag time model is used in the algorithm to correct for differences between blood glucose and interstitial fluid (ISF) glucose concretions (Rebrin et al., 1999). A 10-nm layer of platinum, deposited onto the sensor by sputter coating, serves to prevent in vivo oxidation of the indicator phenylboronic acids groups. Platinum catalytically degrades the reactive oxygen species that are otherwise generated by the body's normal wound healing response to sensor insertion and by the body's response to a foreign body (Colvin and Jiang, 2013). A glucose-permeable membrane covers the hydrogel and provides a biocompatible interface.

The sensor contains a custom integrated circuit (Dehennis et al., 2013) that has been fabricated specifically for this application. Additionally, it includes on-board electrically erasable programmable memory (EEPROM) for local configuration storage and production traceability. Its ability to communicate is mediated by a near field communication interface to the external transmitter. The sensor consists of only six electrical parts encased within the

PMMA capsule: the application specific integrated circuit (ASIC), the ferrite antenna, three capacitors for tuning and regulation, and an on board ultraviolet (UV) LED. The sensor does not contain a battery or other stored power source; instead, it is remotely and discretely powered, as needed, by a simple inductive magnetic link between the sensor and the transmitter. On power-up, the LED source is energized for approximately 4 ms to excite the fluorescent indicator. Between readings, the sensor remains electrically dormant and fully powered down.

2.1.2. Body-worn transmitter

The body-worn transmitter is a rechargeable, external device that is worn over the sensor implantation site and that supplies power to the proximate sensor, calculates glucose concentration from data received from the sensor, and transmits the glucose calculation to a smartphone. The wearable transmitter supplies power to the sensor through an inductive link of 13.56 MHz. The transmitter is placed using an adhesive patch or band (i.e., armband, waistband, and wristband). The external transmitter reads measured glucose data from the subcutaneous sensor up to a depth of approximately 2–3 cm. The transmitter powers and activates a measurement sequence every 2 min and then calculates glucose concentrations and trends. This information also enables the transmitter to determine if an alert condition exists, which is communicated to the wearer through vibration and the transmitter's LED. The information from the transmitter is then transmitted for display to a smartphone via a Bluetooth™ low energy link.

2.2. in vivo performance trial

2.2.1. Clinical study design

The study was designed to provide a preliminary evaluation of the sensor in vivo accuracy and CGM system performance. An institutional review board approved the protocol, and all study procedures were conducted in accordance with the principles of Guideline for Good Clinical Practice (1996). Written informed consent was obtained from all patients before study enrollment.

Twelve adult subjects with type 1 diabetes participated. Four subjects underwent placement of one sensor in the wrist as well as placement of another sensor in the contralateral upper arm (identification [ID] numbers 1–4). Another four subjects (ID numbers 5–8) underwent placement of one sensor in the upper arm. The remaining four subjects (ID numbers 9–12) underwent placement of one sensor in the upper arm as well as placement of another sensor in the abdomen. All subjects had sensors inserted on day 0 and removed on approximately day 28. Subjects attended six in-clinic read sessions (8+ hours each) within that time interval. During the in-clinic visits, a transmitter was placed over each sensor for the collection of sensor data every 2 min. Further, a catheter was placed into an antecubital vein during the in-clinic visits, and venous blood was obtained every 15 min for blood glucose measurements with an YSI blood glucose analyzer (YSI; Model 2300, Yellow Springs, Ohio). Subjects were provided meals and snacks at the clinical site.

Sensor glucose values were not displayed to the subjects or clinicians throughout the duration of this study. All subjects completed the entire 28-day study period. One sensor (in subject 9) failed to send readable data to the transmitter post-insertion due to disconnect of an electrical component (i.e., ASIC pin) within the sensor, and the decision was made to remove the sensor on the next follow-up clinic visit. Therefore, data from a total of 19 sensors among 12 subjects were analyzed in this study.

Glucose measurements were collected via: (1) CGM every 2 min; (2) venous blood sampling and YSI blood glucose analyzer measurements every 15 min and (3) finger-stick glucose measurements pre-prandially and post-prandially. CGM sensor glucose accuracy was assessed by comparison with the YSI blood glucose measurements. A subset of subjects wore the transmitter at home for up to 2 weeks to appraise CGM performance in an ambulatory setting.

2.2.2. Subjects

Enrolled subjects ranged in age from 23 to 64 years (mean = 44 ± 4 years) and included 11 men and one woman. All individuals had been diagnosed with type 1 diabetes for at least 2 years, and BMI ranged from 19.8 to 32.1 kg/m^2 (mean = 27.8 ± 1.0 kg/m^2). Baseline HbA1c ranged from 7.0 to 9.0 (mean = 8.1 ± 0.2).

2.2.3. Sensor insertion and removal

The sensors were inserted into the subcutaneous space using aseptic technique via a small incision (~0.8–1.0 cm) made under local anesthesia with lidocaine. Two 5-0 nylon sutures were used to close the wound. A typical insertion time was less than 5 min. Removal of the device (upon completion of the study) was also performed using aseptic techniques under local anesthesia with lidocaine. A small incision was made at the proximal end of the sensor location, and manual pressure was applied to the distal end to extrude the sensor from the subcutaneous space through the incision. A thin adhesive strip or suture was applied to assure closure at the removal site. Typical excision times were also less than 5 min.

2.2.4. Sensor calibration

The clinical trial was conducted with the glucose display blinded to the subject and clinician. For calibration, the sensor measurements were downloaded from the transmitter along with the subject's finger-stick (SMBG) meter blood glucose measurements. Those finger-stick measurements were prospectively used to calibrate the sensor following the identical calibration regimen as that used for the unblinded system. The calibration regimen for this trial had three phases:

(1) A blinded warm up phase, which comprised the first 24 h after implantation during which glucose levels were not calculated.
(2) Initialization phase, which started at 24 h after implantation and ended after acquiring four calibration points separated by a minimum of 2 h.
(3) Calibration-update phase, which started after the initialization phase and ended after acquiring two calibration points within a single day separated by a minimum of 8 h.

Calibration points were also limited to glucose readings > 60 mg/dL and < 300 mg/dL during rates of glucose change less than 2.5 mg/dL/min.

3. Results

3.1. in vivo accuracy

The mean absolute relative difference (MARD) between CGM and time-matched YSI blood glucose measurements were calculated for all sensors at each in-clinic session and cumulatively over the entire 28-day trial. Glucose data from the six in-clinic sessions of subject 11 (Fig. 3) illustrates how CGM sensor glucose measurements tracked with blood glucose measurements from the YSI. Quantitative comparison of time-matched CGM versus YSI-based glucose measurements (every 15 min) for the in-clinic sessions across all sensors showed a MARD of 11.6 ± 0.7% (Table 1), which is comparable to or lower than the MARDs reported for other commercially available

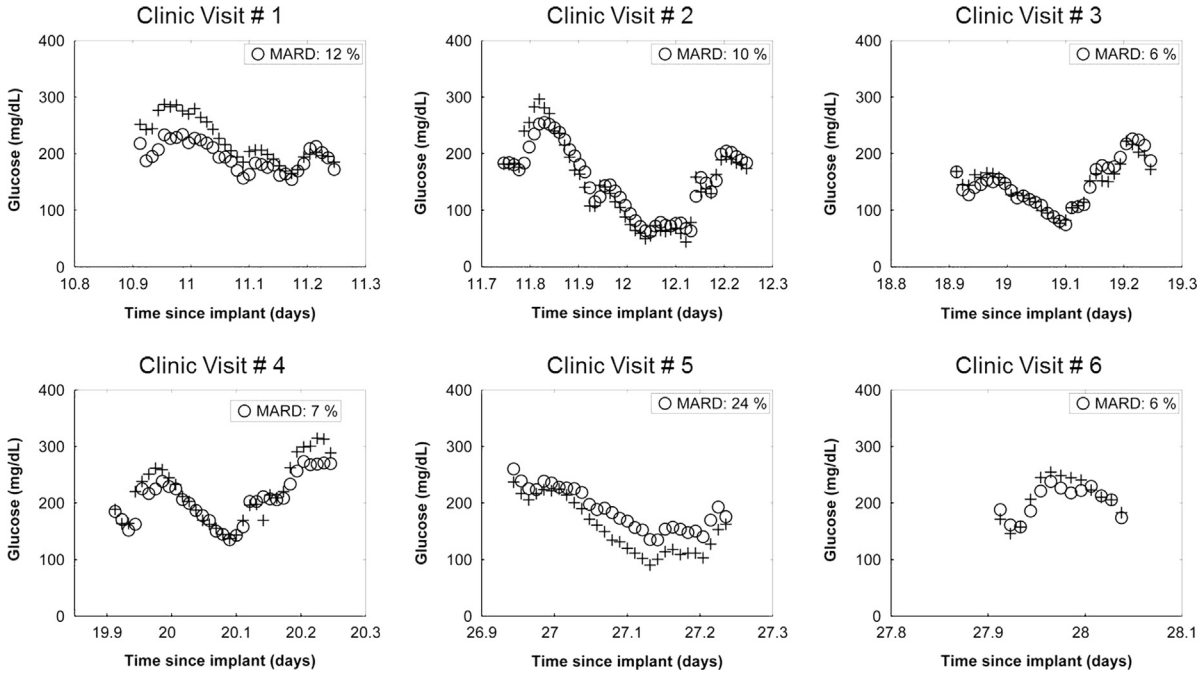

Fig. 3. Paired continuous glucose monitor (open circles) and YSI blood glucose analyzer (crosses) glucose measurements obtained during the six in-clinic visits of subject 11. Overall mean absolute relative difference (MARD) from this sensor (♯2278) was 11.3%, which is comparable to the 19-sensor study average of 11.6%.

Table 1
Continuous glucose monitoring system accuracy for all sensors used in this study.

Subject ID	Sensor ♯	Implant location	MARD* (%)	MAD** (mg/dL)
1	2100	Arm	10.3	11.6
1	2101	Wrist	12.9	14.3
2	2102	Wrist	13.7	15.7
2	2103	Arm	8.2	15.8
3	2105	Wrist	11.6	41.3
3	2104	Arm	12.1	12.9
4	2108	Wrist	17.6	8.1
4	2106	Arm	14.4	7.9
5	2143	Arm	9.3	9.7
6	2155	Arm	8.4	28.3
7	2157	Arm	11.3	6.4
8	2158	Arm	7.8	0.3
9	2271	Abdomen	10.8	–
10	2272	Arm	15.9	38.9
10	2276	Abdomen	11.6	5.1
11	2278	Arm	11.3	12.8
11	2269	Abdomen	11.8	20.2
12	2273	Arm	12.5	–
12	2288	Abdomen	9.6	–
Study average (standard deviation)			11.6 (0.7)	14.9 (1.2)

* Mean absolute relative difference (MARD) was calculated for glucose values > 75 mg/dL.

** Mean absolute difference (MAD) was calculated for glucose values < 75 mg/dL. No MAD values are reported when there were insufficient numbers of YSI to CGM matched pairs below 75 mg/dL.

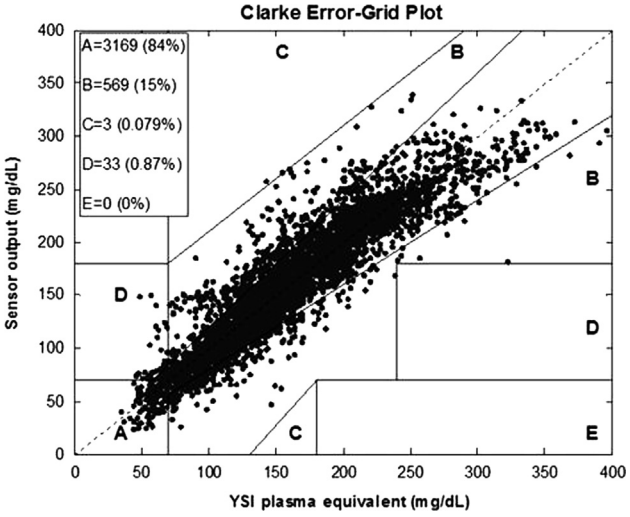

Fig. 4. Clarke error grid analysis of all glucose measurements obtained during in-clinic read sessions. Zone A values are considered clinically accurate, zone B are benign errors, zone C is characterized as the potential for over correction, zone D describes the potential for delayed treatment, and zone E is clinical errors.

sensors (Calhoun et al., 2013; Christiansen et al., 2013; Damiano et al., 2013; McGarraugh et al., 2011). Mean absolute difference (MAD) between YSI and CGM measurements, calculated for all glucose values < 75 mg/dL, was 14.9 mg/dL across all sensors.

Clarke error grid analysis was used to assess the clinical accuracy of all trial data provided by CGM sensors (Clarke and Kovatchev, 2007). A total of 3774 paired data points were obtained to evaluate sensor performance; 99% are within the combined A+B zones, 1% of the data points were in the combined C+D zones and no points are in zone E (Fig. 4). The correlation coefficient between CGM sensor and YSI glucose measurements was 0.926.

3.2. Home-wear glucose measurements

A subset of four subjects (ID numbers 9–12) wore the blinded transmitter continuously at home for approximately 2 weeks in addition to their in-clinic visits. The home use of the CGM system followed the same SMBG calibration updates as was done in the clinic. For data comparison analysis, up to seven SMBG readings were collected by subjects during each home-use day. CGM glucose measurements obtained during home use were indistinguishable from those obtained while in the clinic (Fig. 5). The CGM measurements continued to track well with the discrete blood

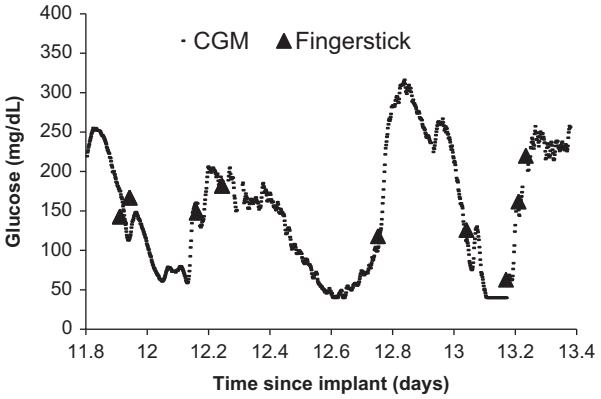

Fig. 5. Sensor glucose data from subject 11 showing the seamless transition in data collected within the clinic (time = 11.8–12.3 days) and after leaving the clinic (time 12.3–13.4 days). Two hyperglycemic and two hypoglycemic episodes were captured by the continuous measurements but not by the SMBG measurements.

glucose measurements and importantly, captured episodes of hyperglycemia and hypoglycemia that were not detected by SMBG. Since gold-standard glucose measurements (i.e., via YSI analyzer) could not be obtained during home wear, the accuracy of the CGM was not assessed for the home-wear period.

4. Discussion

A conspicuous advantage of this abiotic, fluorescent CGM system over existing commercial CGM devices is the significant increase in sensor longevity. Sensors performed throughout the entire 28 day clinical trial, whereas commercially available transcutaneous CGM systems such as the Abbott Navigator, the Medtronic Enlite, and the DexCom G4 Platinum, last only 5, 6 and 7 days, respectively. The in vivo lifespan of those devices may be limited because their sensors utilize enzymes that have a limited life due to thermal degradation (Ginsberg, 2007). By contrast, the Senseonics CGM sensor detects glucose via a non-enzymatic (i.e., bis-boronic acid indicator) methodology that is not subject to degradation and the stability limitations inherent to enzyme-based systems. Further, because the commercial CGM sensors measure current generated at the surface of an electrode, they are highly subject to surface fouling phenomena (i.e., biofouling) which can change electrode surface characteristics and degrade performance. A fluorescent hydrogel-based sensor is not subject to the same degree of fouling because the fluorescent signal emanates from throughout the entire bulk of the hydrogel, not just at the surface. Finally, transcutaneous sensors of other CGM systems protrude from the skin and do not allow for resolution of an acute inflammatory response, thereby limiting sensor accuracy and performance. The Senseonics sensor is fully inserted into the interstitial tissue, thus allowing the body to heal the insertion wound and resolve the acute inflammatory response. In fact, a report of an enzymatic and fully implantable CGM sensor showed performance in a pig model lasting over a year, suggesting full implantation may be important to longevity (Gough et al., 2010).

The MARD of 11.6 ± 0.7% for the abiotic, fluorescent CGM system used in the present 28-day study is comparable or superior to that reported with commercial CGMs of much shorter (up to 7 day) useful lifetimes (Calhoun et al., 2013; McGarraugh et al., 2011). For example, Damiano and colleagues performed a comparative investigation of three commercially available CGM systems in six subjects with type 1 diabetes who underwent 51-h closed-loop blood glucose control experiments in the hospital. Glucose measurement accuracy, as assessed by MARDs, of the FreeStyle Navigator® CGM, DexCom™ SEVEN® CGM, and Medtronic CGM were 11.8 ± 11.1%, 16.5 ± 17.8% and 20.3 ± 18.0%, respectively (Damiano et al., 2013).

5. Conclusions

This preliminary clinical evaluation demonstrated that a fully implantable sensor that utilizes an abiotic recognition mechanism and fluorescence-sensing technology is capable of measuring interstitial glucose continuously throughout a 28-day clinical trial. Sensor measurement accuracy (using a YSI blood glucose analyzer as a benchmark) was comparable or better than that reported for other commercially available CGM devices. Performance throughout the entire duration of the study indicates that much longer durations of use may be possible and demonstrates a potential for a marked increase in sensor in vivo longevity over existing CGMs. Clinical studies of longer durations will further characterize sensor longevity.

Acknowledgments

This study was funded by Senseonics, Incorporated, a privately held company. The authors wish to thank Mr. Ravi Rastogi for his assistance in the preparation of figures for this manuscript and Mr. Steve Walters for clinical study management.

References

Battelino, T., Phillip, M., Bratina, N., Nimri, R., Oskarsson, P., Bolinder, J., 2011. Diabetes Care 34 (4), 795–800.
Calhoun, P., Lum, J., Beck, R.W., Kollman, C., 2013. Diabetes Technol. Ther. 15 (9), 758–761.
Christiansen, M., Bailey, T., Watkins, E., Liljenquist, D., Price, D., Nakamura, K., Boock, R., Peyser, T., 2013. Diabetes Technol. Ther. 15 (10), 1–8.
Clarke, W.L., Kovatchev, B., 2007. J. Diabetes Sci. Technol. 1 (5), 669–675.
Colvin, A.E., Jiang, H., 2013. J. Biomed. Mater. Res. A 101A (5), 1274–1282.
Damiano, E.R., El-Khatib, F.H., Zheng, H., Nathan, D.M., Russell, S.J., 2013. Diabetes Care 36 (2), 251–259.
Dehennis, A.D., Mailand, M., Grice, D., Getzlaff, S., Colvin, A.E., 2013. IEEE International Solid-State Circuits Conference Digest of Technical Papers (ISSCC), pp. 298–299.
Farmer, A., Wade, A., Goyder, E., Yudkin, P., French, D., Craven, A., Holman, R., Kinmonth, A.-L., Neil, A., 2007. Br. Med. J. 335 (7611), 132–135.
Ginsberg, B.H., 2007. J. Diabetes Sci. Technol. 1 (1), 117–121.
Gough, D.A., Kumosa, L.S., Routh, T.L., Lin, J.T., Lucisano, J.Y., 2010. Sci. Transl. Med. 2 (42), 1–8.
Group, U.P.D.S.U., 1998. Lancet 352, 837–853 (1998/09/22 ed.).
Guideline for Good Clinical Practice, 1996. International Conference on Harmonization, E6 (R1).
James, T.D., Phillips, M.D., Shinkai, S., 2006. Boronic Acids in Saccharide Recognition. The Royal Society of Chemistry, Cambridge, UK.
Klonoff, D.C., 2007. J. Diabetes Sci. Technol. 1 (1), 130–132.
McGarraugh, G., Brazg, R., Richard, W., 2011. J. Diabetes Sci. Technol. 5 (1), 99–106.
Rebrin, K., Steil, G.M., Van Antwerp, W.P., Mastrototaro, J.J., 1999. Am. J. Physiol. 277, E561–E571.
Resnick, H.E., 2006. Diabetes Care 29 (3), 531–537.
Shibata, S., Heo, Y.J., Okitsu, T., Matsunaga, Y., Kawanishi, T., Takeuchi, S., 2010. Proc. Natl. Acad. Sci. USA 107 (42), 17894–17898.
Wang, X., Mdingi, C., DeHennis, A., Colvin, A.E., 2012. Proceedings of the 34th Annual International Conference of the IEEE Engineering in Medicine and Biology Society, San Diego.
Wild, S., Roglic, G., Green, A., Sicree, R., King, H., 2004. Diabetes Care 27 (5), 1047–1053.